Electronic Supplementary Material (ESI) for Chemical Communications.
This journal is © The Royal Society of Chemistry 2016

Electronic Supplementary Information

$[Au_{25}(SR)_{18}]_2^{2-}$: A noble metal cluster dimer in the gas phase

Ananya Baksi,[†] Papri Chakraborty,[†] Shridevi Bhat,[†] Ganapati Natarajan and Thalappil Pradeep*

DST Unit of Nanoscience (DST UNS) and Thematic Unit of Excellence (TUE),Department of Chemistry, Indian Institute of Technology Madras,Chennai 600 036, India
*Corresponding author: Fax: + 91-44 2257-0545
*E-mail: pradeep@iitm.ac.in

[†]Contributed equally

Experimental Section

Materials:

Tetrahydrofuran (THF), Dichloromethane (DCM), Phenylethanethiol (PET), Dodecanethiol (DDT), Tetraoctyl ammonium bromide (TAOBr), Methanol (MeOH), Sodium borohydride ($NaBH_4$) and Phenylethanethiol (PET)were purchased from Sigma Aldrich. Chloroauric acid ($HAuCl_4$. $3H_2O$) was prepared in lab from pure gold. All the chemicals were used without further purification.

Synthesis of $Au_{25}(PET)_{18}^-$:

About 40 mg of $HAuCl_4.3H_2O$ was taken in 7.5 ml THF and mixed with 65 mg of TAOBr and stirred for around 15 min to get an orange red solution. To the solution,PETwas added in 1:5 molar ratio (68 µL) and stirred for another hour. This resulted in Au-thiolate formation. The as-formed thiolate was then reduced by adding about 39 mg of $NaBH_4$ in ice-cold water. The color changed from yellow to brown. The solution was allowed to stir for another 5 hours for complete conversion and size focusing synthesis of $Au_{25}(PET)_{18}^-$. The as-synthesized cluster was then vacuum dried by rotavapor and precipitated using excess MeOH to get rid of free thiol and excess thiolate. The process was repeated a few times. Then the Au_{25} cluster was extracted into acetone and centrifuged and the supernatant solution was collected leaving behind a precipitate consisting of larger clusters. The acetone solution was vacuum dried. Finally the cluster was dissolved in dichloromethane (DCM) and centrifuged and the supernatant solution was collected which consisted of the pure cluster. The resulted cluster was characterized by UV-vis absorption spectroscopy where characteristic peaks at 675, 450 nm confirmed the formation of Au_{25} clusters. Detailed characterization was by done

by electrospray ionization (ESI) and matrix assisted laser desorption ionization (MALDI) mass spectrometry (MS).

Instrumental Details:

Detailed experiments described in this work were carried out in Waters' Synapt G2Si HDMS instrument. The lab has other mass spectrometers too such as MALDI MS. The Synapt instrument consists of an electrospray source, quadrupole ion guide/trap, ion mobility cell, and TOF detector. A detailed instrumental view is shown in Figure 1 of the main manuscript. Different gases are used in different parts of the instrument. Nitrogen gas is used as nebulizer gas. High pure $N_2$was used inside the ion mobility cell and the ions were directed through a drift tube. To reduce collision induced fragmentation, heliumwas used as the curtain gas before the ions entered the mobility cell. High pure Ar gas was used for collision induced dissociation (CID).All the experiments were done in negative ion mode. At standard condition, to obtain monomeric $Au_{25}(PET)_{18}^-$mass spectrum in ion mobility (ESI IM MS) mode, the following instrumental parameters were used:

Sample concentration: 1µg/mL
Solvent: DCM
Flow Rate: 10-20 µL/min
Capillary Voltage: 2-3 kV
Cone Voltage: 120-150 V
Source Offset: 80-120 V
Desolvation gas flow: 400 L/h
Trap gas flow: 5 mL/min
He gas flow: 100 mL/min
Ion mobility gas flow: 50 mL/min
Bias Voltage: 45 V
Wave Velocity: 400 m/s
Wave Height: 40 V

To obtain dimer and other polymers of $Au_{25}(PET)_{18}^-$, following parameterswere followed:

Capillary Voltage: 1-2 kV
Cone Voltage: 0-50 V
Source Offset: 0-20 V
Desolvation gas flow: 400 L/h
Trap gas flow: 5-10 mL/min
He gas flow: 100-180 mL/min
Ion mobility gas flow: 50-70 mL/min
Bias Voltage: 25-30 V

Rest of the parameters were kept the same as before.

UV-vis absorption studies were conducted with a Perkin Elmer Lambda25 instrument with 1 nm band pass.

Electronic Supplementary Information 1

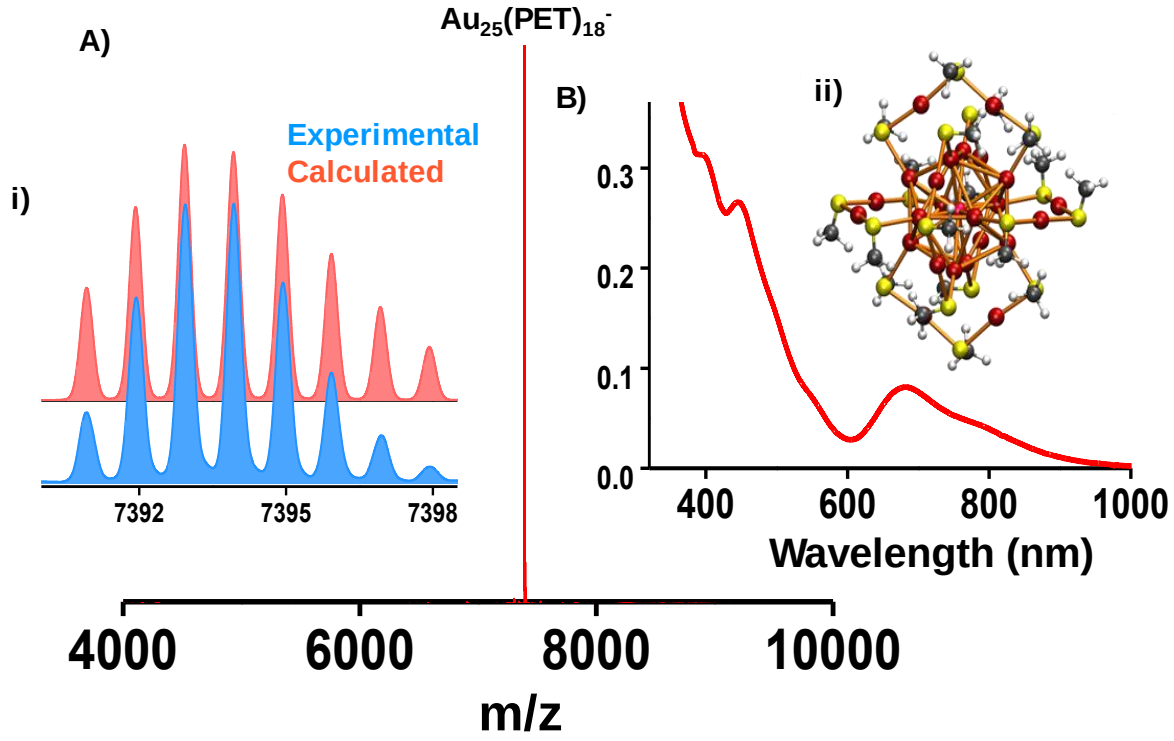

Figure S1: A) ESI MS of $Au_{25}(PET)_{18}^-$showing a single peak centred at m/z 7393 (average mass). Experimental isotope pattern of this peak is matching well with the calculated one as shown in inset i). B) UV-vis absorption spectrum of $Au_{25}(PET)_{18}^-$ showing characteristic peaks conforming successful synthesis. Density functional theory (DFT) optimized structure of the cluster is shown in the inset ii). Ligands were replaced with –SMe, to reduce the computational demand.

Electronic Supplementary Information 2

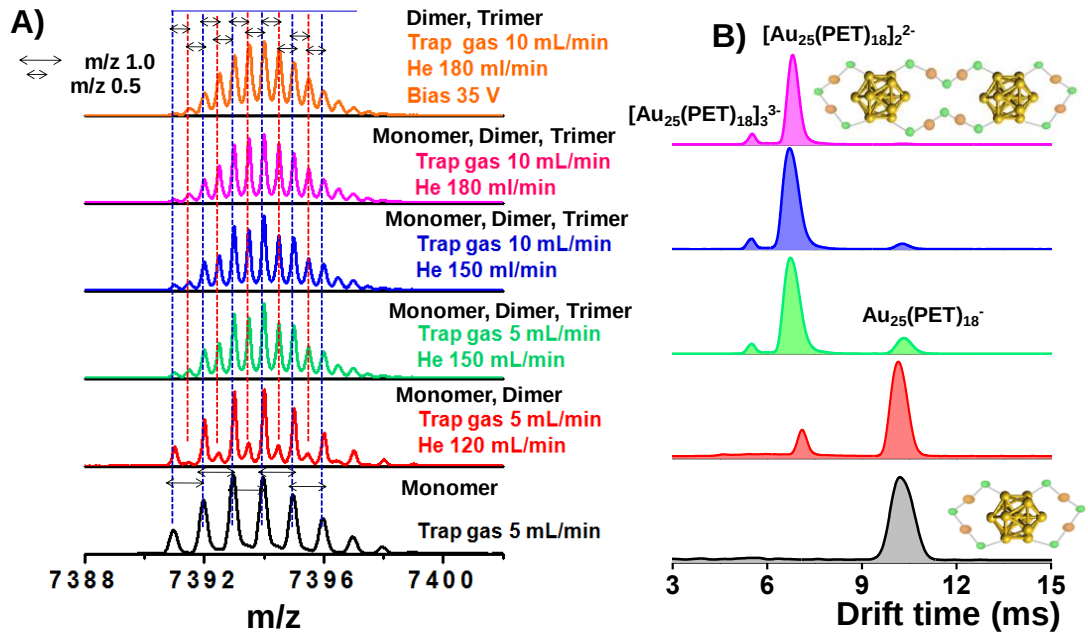

Figure S2: A) Optimization of different gas flow rates to obtain $[Au_{25}(PET)_{18}]_2^{2-}$ and B) corresponding drift time plots. Schematic representation of the structures is also shown.

Electronic Supplementary Information 3

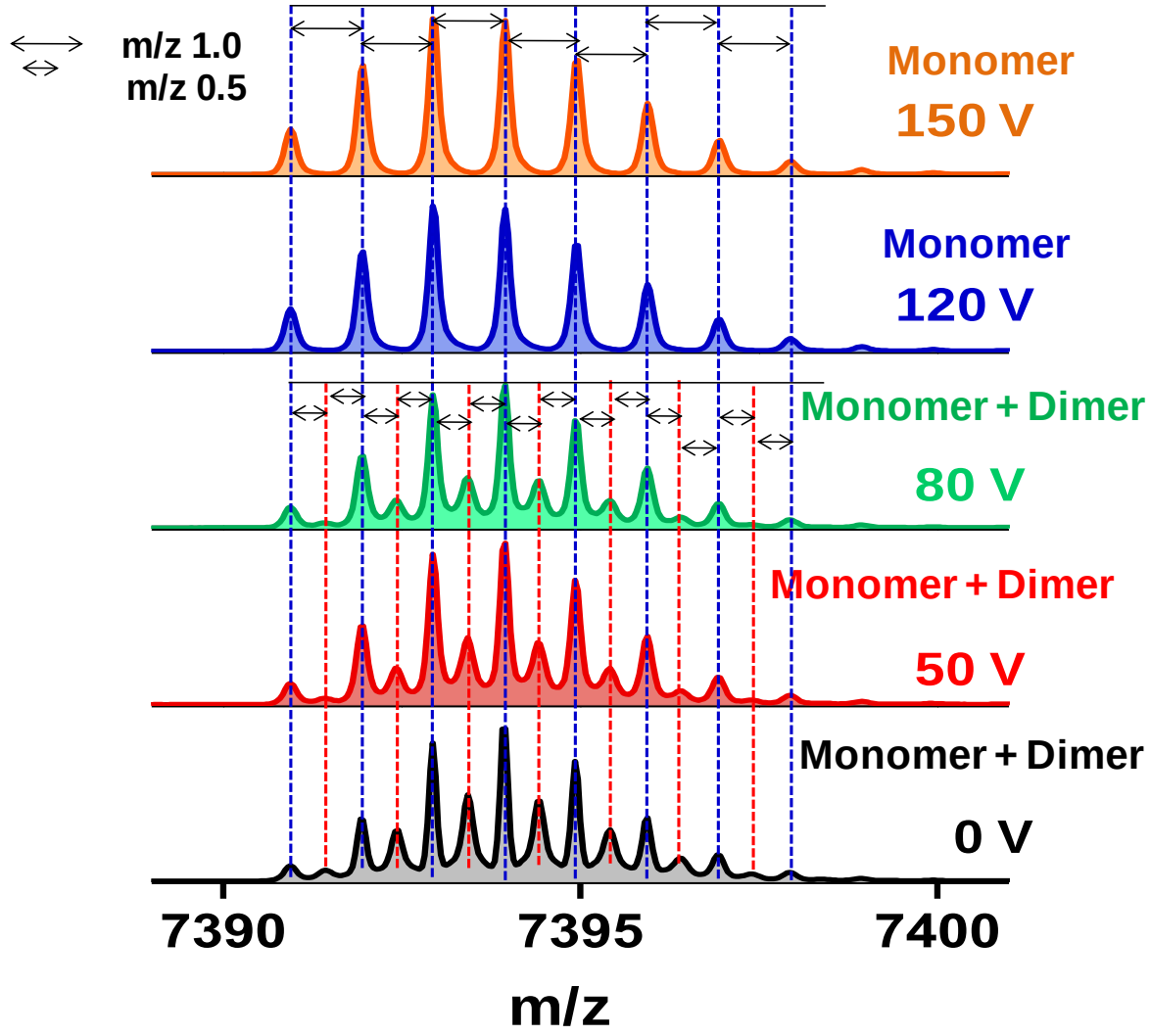

Figure S3: Cone voltage dependence for dimer formation in case of $Au_{25}(PET)_{18}^-$. Dimers are formed at lower cone voltages.

Electronic Supplementary Information 4

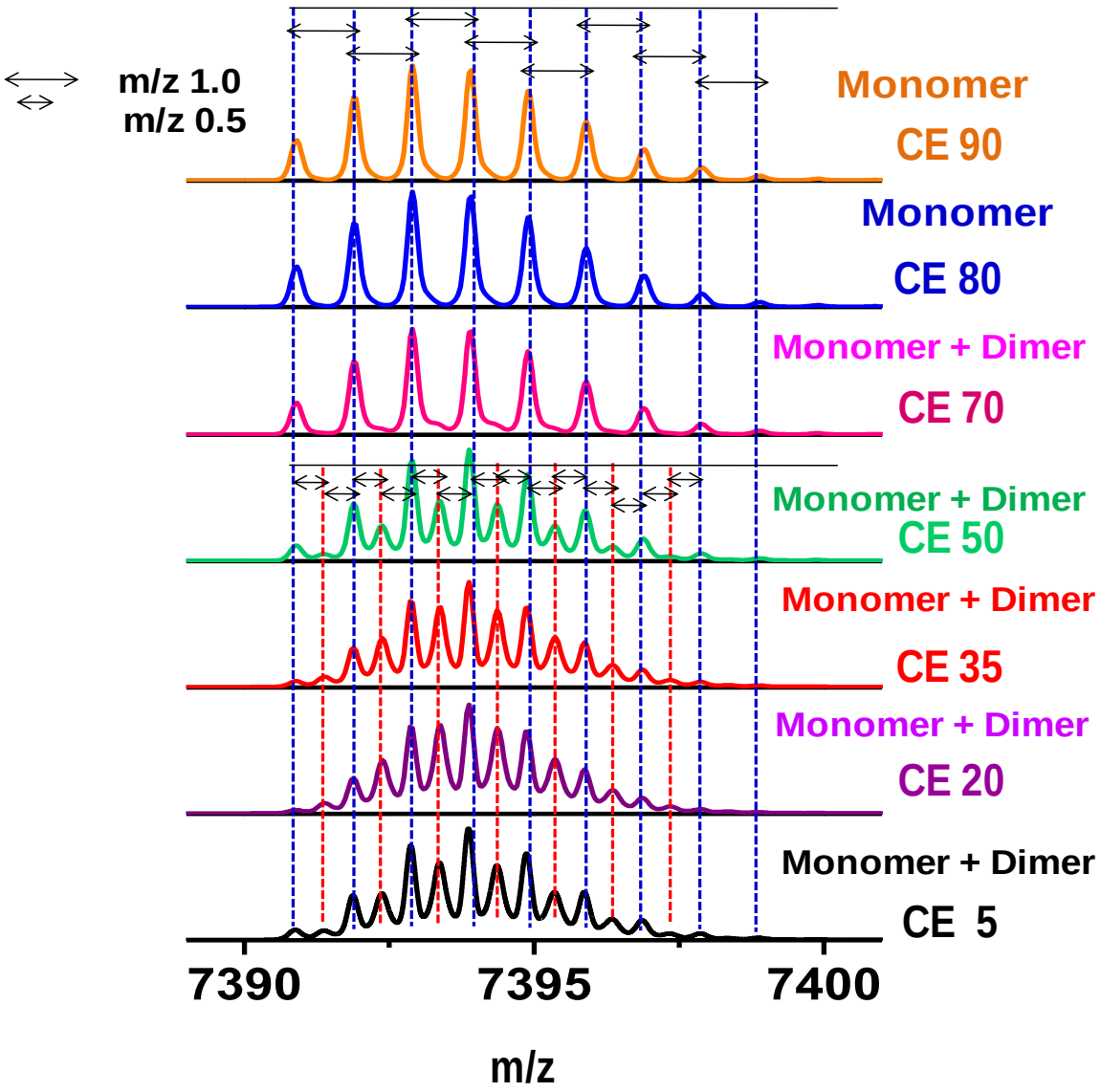

Figure S4: Formation of monomer from dimer upon gradually increasing the collision energy in the case of $Au_{25}(PET)_{18}^-$.

Electronic Supplementary Information 5

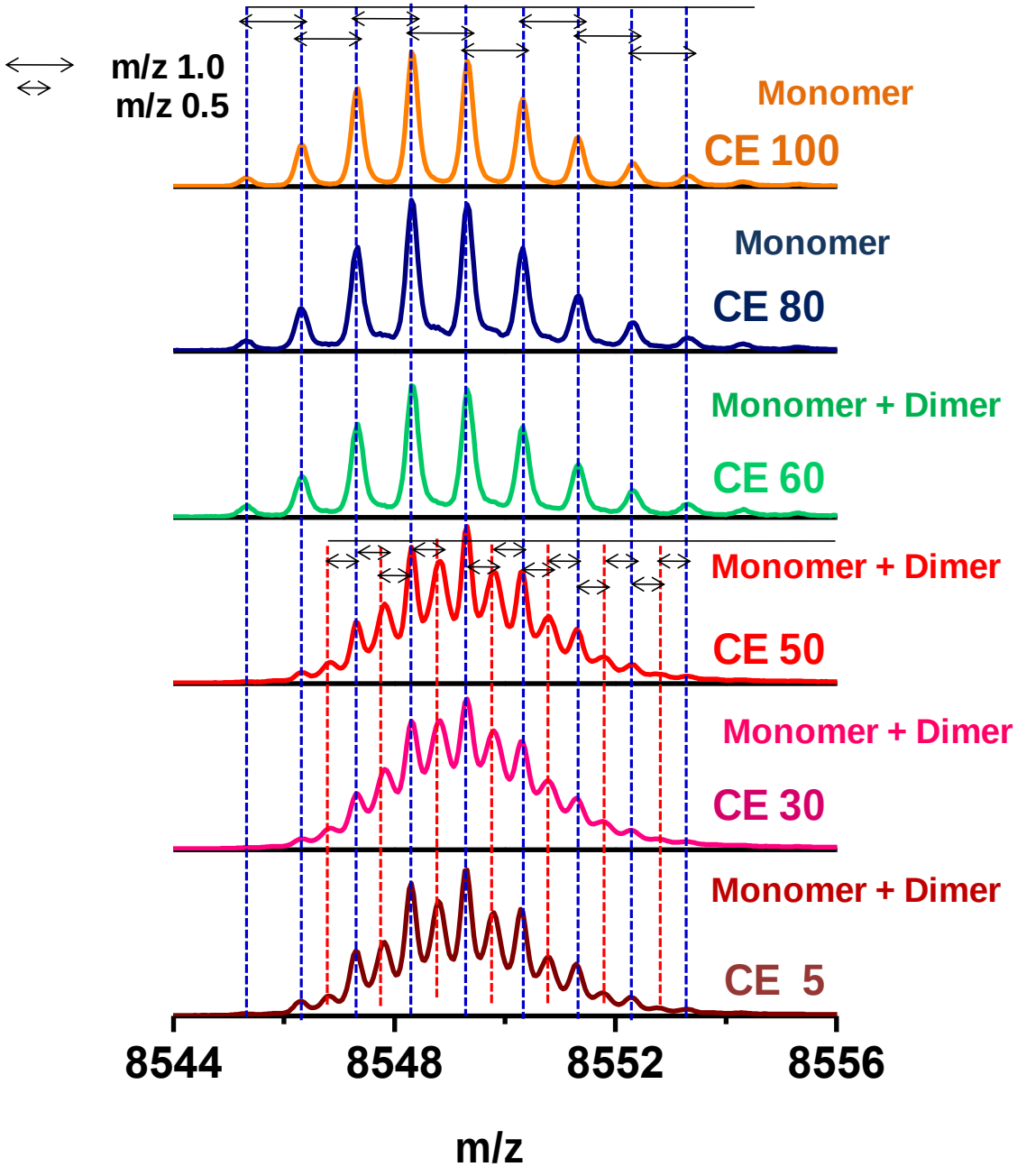

Figure S5: Formation of monomer from dimer upon gradually increasing the collision energy in the case of $Au_{25}(DDT)_{18}^-$.

Electronic Supplementary Information 6

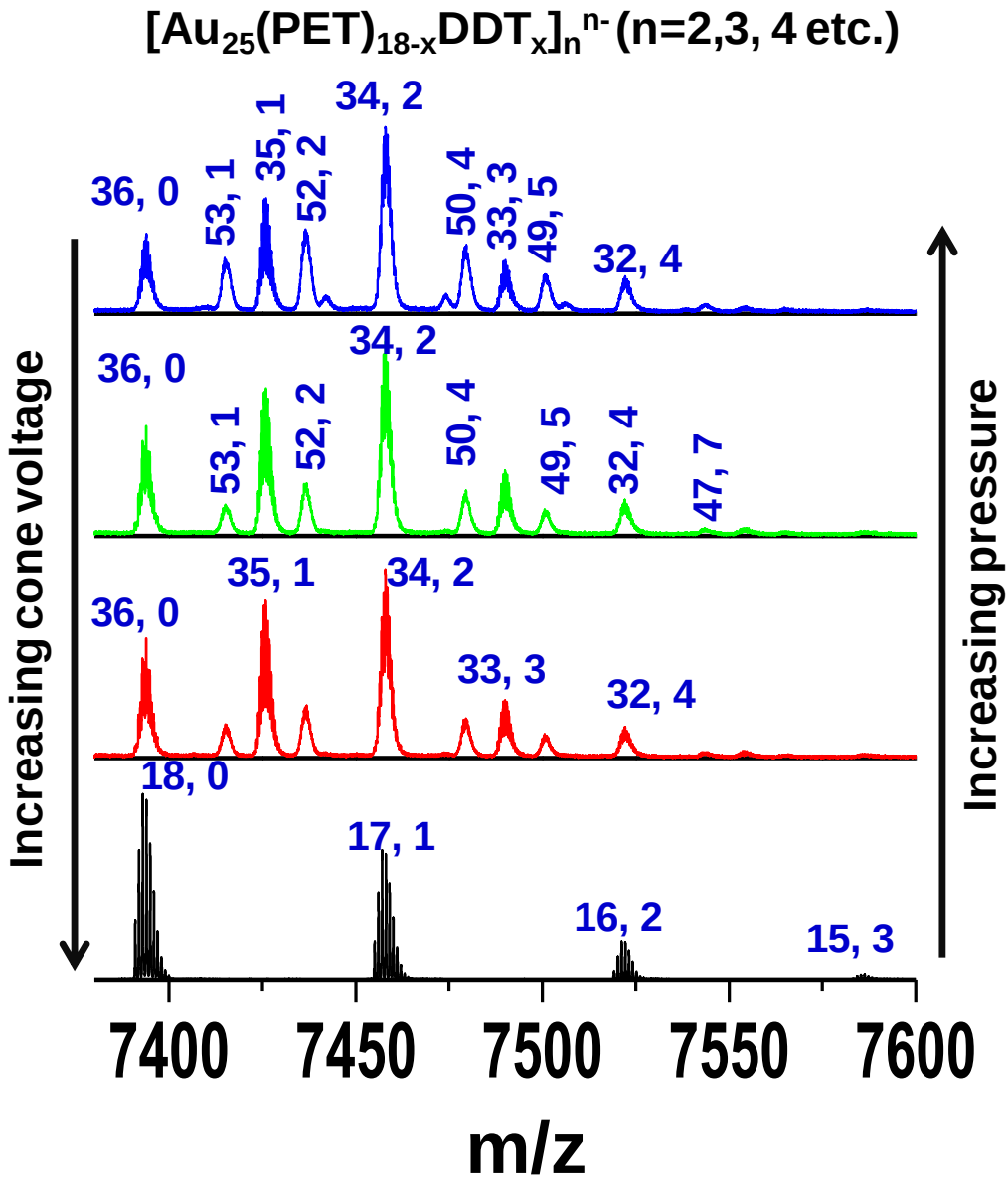

Figure S6: Cone voltage and pressure dependence in case of ligand exchange of PET with DDT.Product peaks are labelled where the first number corresponds to the number of PET in the cluster and the second corresponds to that of DDT.

Electronic Supplementary Information 7

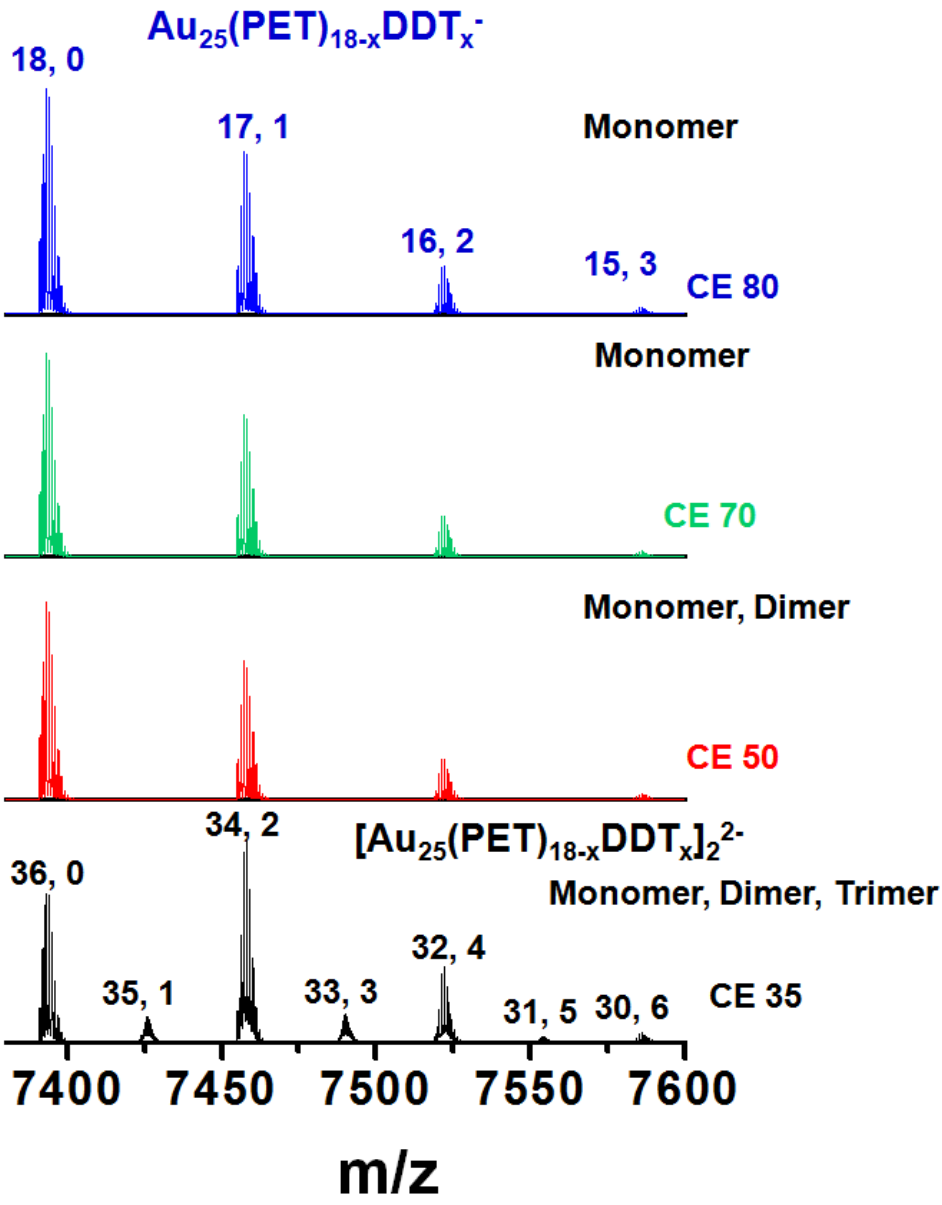

Figure S7: Collision energy dependence in the case of ligand exchange of $Au_{25}(SR)_{18}$ system with DDT showing the formation of monomer from polymers.Product peaks are labelled where the first number corresponds to number of PET in the cluster and the second corresponds to number of DDT. CE corresponds to nominal collision energy.

Electronic Supplementary Information 8

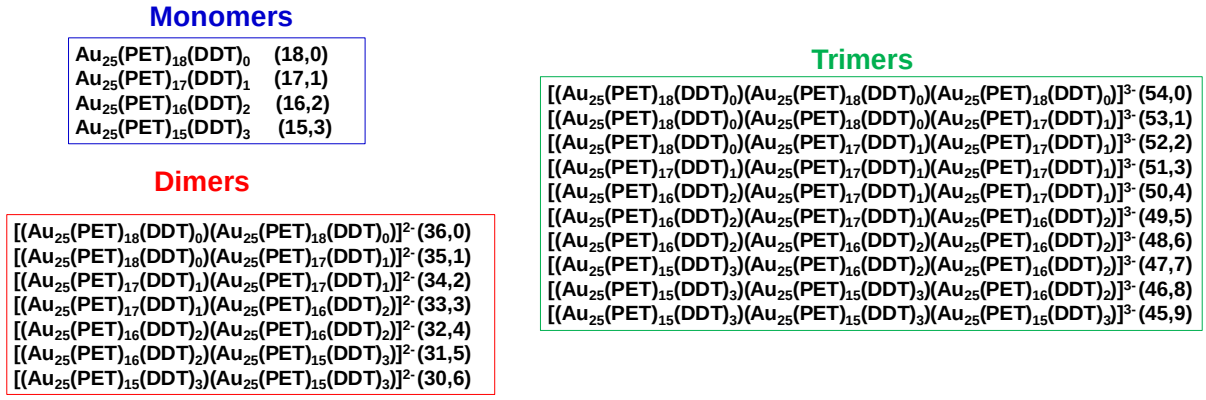

Figure S8: Compositions of different monomers, dimers and trimers formed during ligand exchange and subsequent polymerization process.

Electronic Supplementary Information 9

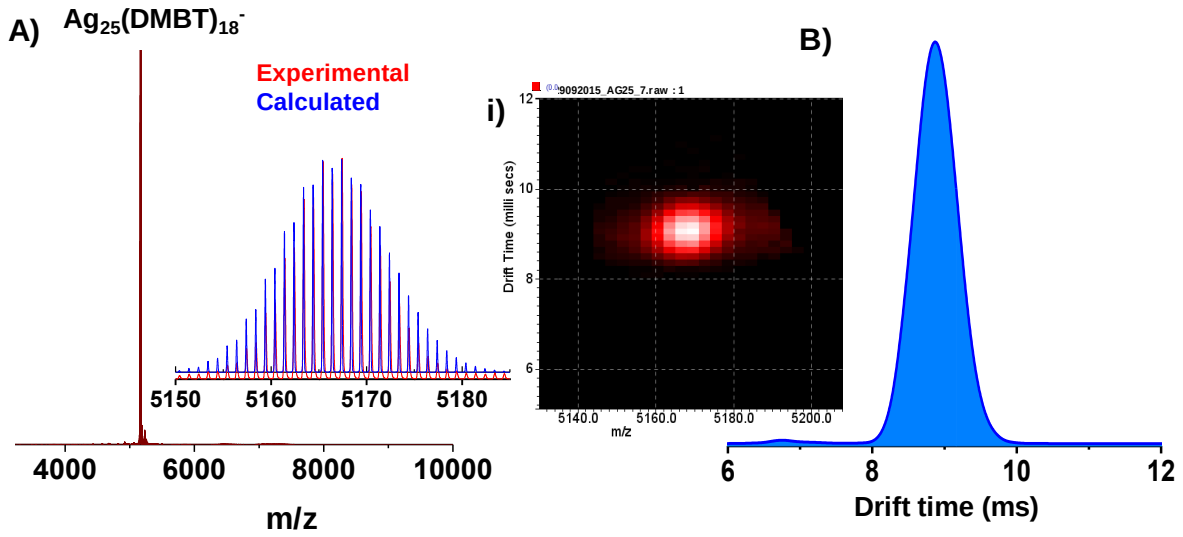

Figure S9: A)ESI MS of $Ag_{25}(DMBT)_{18}$ in negative ion mode showing molecular ion peak. Experimental data are matching well with the calculated spectrum as shown in inset i). B) Drift time profile of the same cluster is showing peak at 8.8 ms. Plot of m/z vs. drift time for $Au_{25}(PET)_{18}$is shown in inset ii).

Computational Details:

We used density functional theory as implemented real-space projector augmented wave method in GPAW[1]. Au($5d^{10}6s^{1}$), and S($3s^{2}3p^{4}$) electrons were treated as valence and the inner electrons were included in a frozen core. The GPAW setups for gold and silver included scalar-relativistic corrections. The exchange-correlation functional employed was the generalized gradient approximation of Perdew, Burke and Ernzerhof (GGA-PBE)[2].

We used a 0.2 Å grid spacing for electron density in all calculations and a convergence criterion of 0.05 eV/Å for the residual forces on atoms was used in all structure optimizations, without any symmetry constraints. For computational efficiency during the structural optimizations, rather than employing the finite-difference real-space grid method for the expansion of the pseudo wave functions, we used instead the LCAO method[3]as implemented in GPAW by employing a double zeta plus polarization (DZP) basis set. For greater precision in our energy calculations, we then recalculated the total energies at this geometry minimum using the finite-difference method in GPAW.

The crystal structures of $Au_{25}(SR)_{18}$[4]were used for building the initial structures of the A, B and C isomers of $[Au_{50}(SR)_{36}]^{2-}$. For efficient computations, we terminated each sulphur atom with a hydrogen atom in all the clusters. The initial structures of isomers A, B and C were first geometry optimized, and then the value of the total energy of each isomer taken at the

geometry-optimized configuration using was recalculated using the more accurate finite-difference method in GPAW. For the binding energy calculation we used the total energy of $Au_{25}(SH)_{18}$ from Ref 5. where they have used the same method of calculation as ours. The structures of the isomers of $Au_{50}(SH)_{36}$ were built up with the help of Avogadro software package[6]and visualizations were created with Visual Molecular Dynamics (VMD) software[7].Coordinates of geometry optimized isomers.

References:

(1) Enkovaara, J.; et al. J. Phys.: Condens. Matter 2010, 22, 253202.
(2) Perdew, J. P.; Burke, K. *Phys. Rev. Lett.* **1996**, *77*, 3865.
(3) Larsen, A. H.; Vanin, M.; Mortensen, J. J.; Thygesen, K. S.; Jacobsen, K. W. *Phys. Rev. B* **2009**, *80*, 195112.
(4) Krishnadas, K. R., Ghosh, A., Baksi, A., Chakraborty, I., Natarajan, G., and Pradeep, T.*J. Am. Chem. Soc.*, **2016**, *138*, 140.

(5) (a) Heaven, M. W.; Dass, A.; White, P. S.; Holt, K. M.; Murray, R. W. *J. Am. Chem. Soc.* **2008**, *130*, 3754. Zhu, M.; Aikens, C. M.; Hollander, F. J.; Schatz, G. C.; Jin, R. *J. Am. Chem. Soc.* **2008**, *130*, 5883.

(6) Hanwell, M.; Curtis, D.; Lonie, D.; Vandermeersch, T.; Zurek, E.; Hutchison, G. *J. Cheminf.* **2012**, *4*, 1.
(7) Humphrey, W.; Dalke, A.; Schulten, K. J. *Mol. Graphics* **1996**, *14*, 33.

Electronic Supplementary Information 10

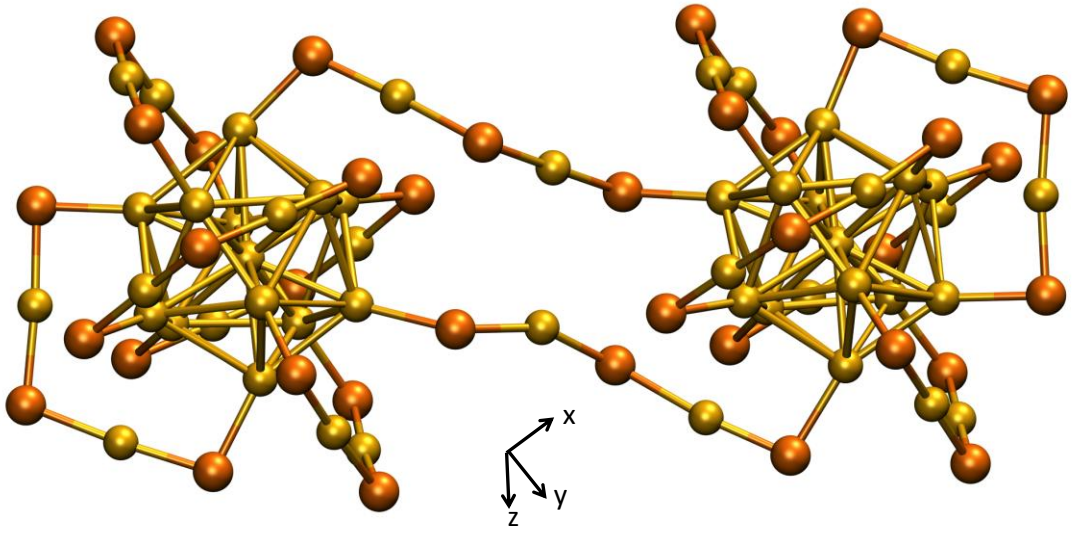

Figure S10: A third possible structural isomer (C) of the $[Au_{50}(SR)_{36}]^{2-}$ dimer considering inter-cluster bonding via Au_2S_3 staples. The DFT-optimized structure of isomer C has linkages formed when the two clusters are positioned so that the edges of the staples are adjacent to each other. The diagonal bonding between the edges of staples on either cluster forms two parallel Au_2S_3 chains linking the two clusters. The view shown is looking in the negative *z*-direction (top view), according to the Cartesian axes shown. The ligand R-groups are removed for clarity and gold atoms are shown in gold and sulphur atoms in orange, using the ball and stick atom representation.

Table S1:*Collision Cross Section values of $Au_{25}(SR)_{18}$ monomer, dimer and trimer.*

Species	CCS value (A°²)
$[Au_{25}(PET)_{18}]^-$	297.8
$[Au_{25}(PET)_{18}]_2^{2-}$	453.4
$[Au_{25}(PET)_{18}]_3^{3-}$	668.3

Table S2: *Collision Cross Section values of $Au_{25}(SR)_{18}$ monomer, dimer and trimer after ligand exchange with DDT.*

Monomers

Species	CCS value (A°²)
$[Au_{25}(PET)_{18}]^-$	303.1
$[Au_{25}(PET)_{17}(DDT)_1]^-$	305.2
$[Au_{25}(PET)_{16}(DDT)_2]^-$	306.7

Dimers

Species	CCS value (A°²)
$[Au_{25}(PET)_{18}]_2^{2-}$	461.2
$[[Au_{25}(PET)_{18}]\ [Au_{25}(PET)_{17}(DDT)_1]]^{2-}$	463.1
$[[Au_{25}(PET)_{17}(DDT)_1][Au_{25}(PET)_{17}(DDT)_1]]^{2-}$	465.4
$[[Au_{25}(PET)_{16}(DDT)_2][Au_{25}(PET)_{17}(DDT)_1]]^{2-}$	467.6
$[[Au_{25}(PET)_{16}(DDT)_2][Au_{25}(PET)_{16}(DDT)_2]]^{2-}$	469.6
$[[Au_{25}(PET)_{15}(DDT)_3][Au_{25}(PET)_{16}(DDT)_2]]^{2-}$	471.5
$[[Au_{25}(PET)_{15}(DDT)_3][Au_{25}(PET)_{15}(DDT)_3]]^{2-}$	472.9

Trimers

Species	CCS value (A°²)
$[Au_{25}(PET)_{18}]_3^{3-}$	665.8
$[[Au_{25}(PET)_{18}]\ [Au_{25}(PET)_{18}]\ [Au_{25}(PET)_{17}(DDT)_1]]^{3-}$	667.4
$[[Au_{25}(PET)_{18}]\ [Au_{25}(PET)_{17}(DDT)_1][Au_{25}(PET)_{17}(DDT)_1]]^{3-}$	668.5
$[[Au_{25}(PET)_{17}(DDT)_1][Au_{25}(PET)_{17}(DDT)_1][Au_{25}(PET)_{17}(DDT)_1]]^{3-}$	670.5
$[[Au_{25}(PET)_{16}(DDT)_2][Au_{25}(PET)_{17}(DDT)_1][Au_{25}(PET)_{17}(DDT)_1]]^{3-}$	671.8
$[[Au_{25}(PET)_{16}(DDT)_2][Au_{25}(PET)_{16}(DDT)_2][Au_{25}(PET)_{17}(DDT)_1]]^{3-}$	673.7
$[[Au_{25}(PET)_{16}(DDT)_2][Au_{25}(PET)_{16}(DDT)_2][Au_{25}(PET)_{16}(DDT)_2]]^{3-}$	675.6
$[[Au_{25}(PET)_{15}(DDT)_3][Au_{25}(PET)_{16}(DDT)_2][Au_{25}(PET)_{16}(DDT)_2]]^{3-}$	676.9
$[[Au_{25}(PET)_{15}(DDT)_3][Au_{25}(PET)_{15}(DDT)_3][Au_{25}(PET)_{16}(DDT)_2]]^{3-}$	677.8
$[[Au_{25}(PET)_{15}(DDT)_3][Au_{25}(PET)_{15}(DDT)_3][Au_{25}(PET)_{15}(DDT)_3]]^{3-}$	679.6

Table S3: *Isomers of $[Au_{50}(SH)_{36}]^{2-}$. The DFT energies of the three isomers A, B, C, their binding energies and binding energy difference with respect to isomer A are shown. The value of the monomer energy -220.28 eV was taken from Ref. 17 in the main article (K. R. Krishnadas, A. Ghosh, A. Baksi, I. Chakraborty, G. Natarajan and T. Pradeep, J. Am. Chem. Soc., 2016,* ***138****, 140-148.)*

Isomer	Energy/eV	Binding Energy (E_b)/eV	E_b-E_b(A)/eV
A	-439.385	+1.18	0.00
B	-439.068	+1.49	+0.31
C	-438.200	+2.36	+1.18